Journal of Alloys and Compounds 408–412 (2006) 976–980

Journal of ALLOYS AND COMPOUNDS

www.elsevier.com/locate/jallcom

Structural comparison in a series of 3,5-bis(2-pyridyl)pyrazolato bridged Ln(III)–Cr(III) dinuclear complexes

Ryouji Kawahata, Toshiaki Tsukuda, Takashi Yagi, Akira Fuyuhiro, Sumio Kaizaki *

Department of Chemistry, Graduate School of Science, Osaka University, Toyonaka, 560-0043 Osaka, Japan

Received 28 July 2004; received in revised form 2 December 2004; accepted 2 December 2004

Abstract

The novel Ln^{III} ion size dependent structural transformation round Ln^{III} in a series of discrete $[(hfac)_3Ln(\mu\text{-bpypz})Cr(acac)_2]$ dinuclear complexes is examined in comparison with the structural parameters in relation to the lanthanide(III) ion radius.

Keywords: Ln–Cr dinuclear complexes; X-ray structures; Structural parameters

---

1. Introduction

There is the ion size dependent change of the coordination number (CN) for isoleptic Ln^{III} complexes such as $[Ln(hfac)_3(bpy\text{ or }phen)_n]$(hfac = hexafluoromethylacetylacetonate: from $n = 1$(Yb) to 2(La)) [1]. In mononuclear complexes with the identical CN, the structural modification by the ion size has recently been studied by Mizukami et al. where fine helical structural adjustment by the Ln ion size was postulated leading to intentional control of helices or sheets in nanostructures [2]. In addition, the structural variations of macrocyclic Ln^{III}(DOTA) complexes were demonstrated by Bombieri and co-workers [3]. In our recent study, only subtle polyhedral change in a series of $[Ln(hfac)_3(IM2py)]$ was reported [4], whereas polyhedral variation with CN change from 7 to pseudo 8 was discovered in a series of 4f–4f dinuclear complexes $[(HBpz_3)Ln(\mu\text{-pba})_4Ln(HBpz_3)]$(pba = *S*- and *R*-phenylbutyrate) [5]. On the other hand, the 3d–4f heteropolymetallic complexes has been extensively studied to improve physicochemical properties with much interest [6]. No significant structural change was found in our three series of 3d–4f trinuclear $[Ni(\mu\text{-tdo or -edo})\{Ln(HBpz_3)_2\}_2]$ [7] and dinuclear $[(acac)_2Cr(\mu\text{-ox})Ln(HBpz_3)_2]$ [8–10]. In contrast, there seem to be little Ln ion size dependent structural variations not only in kinetically inert optically active Cr^{III}–Ln^{III} self-assembled triple-stranded podates [11], but also in the podate Fe^{II}–Ln^{III} complexes even associated with the fine control of the Fe (II) spin-state equilibrium [12]. Comparison of different configurations along a series of 3d–4f dinuclear complexes is expected to provide invaluable information on integrated intramolecular interactions in relation with physicochemical properties including chiroptical spectra.

This paper will report structural comparison of stereochemistry of new discrete bpypz bridged Ln–Cr dinuclear complexes $[(hfac)_3Ln(\mu\text{-bpypz})Cr(acac)_2]$ (Ln = Ce(**1**), Nd(**2**), Sm(**3**), Gd(**4**), Dy(**5**), Er(**6**), Yb(**7**)). The novel structural transformation has been already communicated elsewhere [13].

2. Experimental

2.1. Preparation of the complexes

$[Cr(acac)_2(bpypz)] \cdot C_2H_5OH$

To an ethanol solution (100 ml) of $[Cr(acac)_2(H_2O)_2]Cl$, Hbpypz (5 mmol) was added and stirred for a day at room temperature. This solution was concentrated on a

---

* Corresponding author. Fax: +81 6 6850 5408.
E-mail address: kaizaki@chem.sci.osaka-u.ac.jp (S. Kaizaki).

0925-8388/$ – see front matter
doi:10.1016/j.jallcom.2004.12.146

Table 1
Elemental analyses of $[(hfac)_3Ln(\mu\text{-bpypz})Cr(acac)_2]$

	Complexes	C (%)	H (%)	N (%)
1	Cr(μ-bpypz)Ce	37.21 (37.03)	2.04 (2.13)	4.63 (4.55)
2	Cr(μ-bpypz)Nd	36.70 (36.90)	2.04 (2.12)	4.54 (4.53)
3	Cr(μ-bpypz)Sm	36.56 (36.72)	2.00 (2.11)	4.63 (4.51)
4	Cr(μ-bpypz)Gd	35.67 (36.52)	2.05 (2.10)	4.49 (4.48)
5	Cr(μ-bpypz)Dy	36.33 (36.37)	2.08 (2.09)	4.53 (4.46)
6	Cr(μ-bpypz)Er	36.28 (36.23)	1.99 (2.08)	4.49 (4.45)
7	Cr(μ-bpypz)Yb	36.05 (36.06)	1.99 (2.07)	4.49 (4.43)

Calculated values are given in parentheses.

vacuum rotatory evaporator and added acetonitrile (50 ml), then the pink powder precipitated. This pink precipitate ($[Cr(acac)_2(Hbpypz)]Cl$) was filtered off, washed three times with acetone and dried under vacuum. To an ethanol solution (10 ml) of the above pink precipitate (2 mmol) was added Et_3N (2 mmol) and the mixture was stirred for a while. Then orange powder precipitated, and it was filtered off, washed several times with ethanol. Anal. Calcd. for $C_{23}H_{29}O_5N_4Cr_1$ ($[Cr(acac)_2(bpypz)]\cdot C_2H_5OH$): C, 58.02; H, 5.65; N, 10.83. Found: C, 57.53; H, 5.52; N, 10.88%.

$[(hfac)_3Ln(\mu\text{-bpypz})Cr(acac)_2]$ (Ln = Ce(1), Nd(2), Sm(3), Gd(4), Dy(5), Er(6), Yb(7))

All $[(hfac)_3Ln(\mu\text{-bpypz})Cr(acac)_2]$ dinuclear complexes were prepared by the following method. To a chloroform solution (10 ml) of $[Cr(acac)_2(bpypz)]\cdot C_2H_5OH$ (0.2 mmol), was added $[Ln(hfac)_3(H_2O)_2]$ (0.2 mmol) and the mixture was stirred for a day. A small amount of hexane was added to this solution and evaporated slowly. Violet crystals except for the brown complex **1** were obtained. The elemental analyses are given in Table 1.

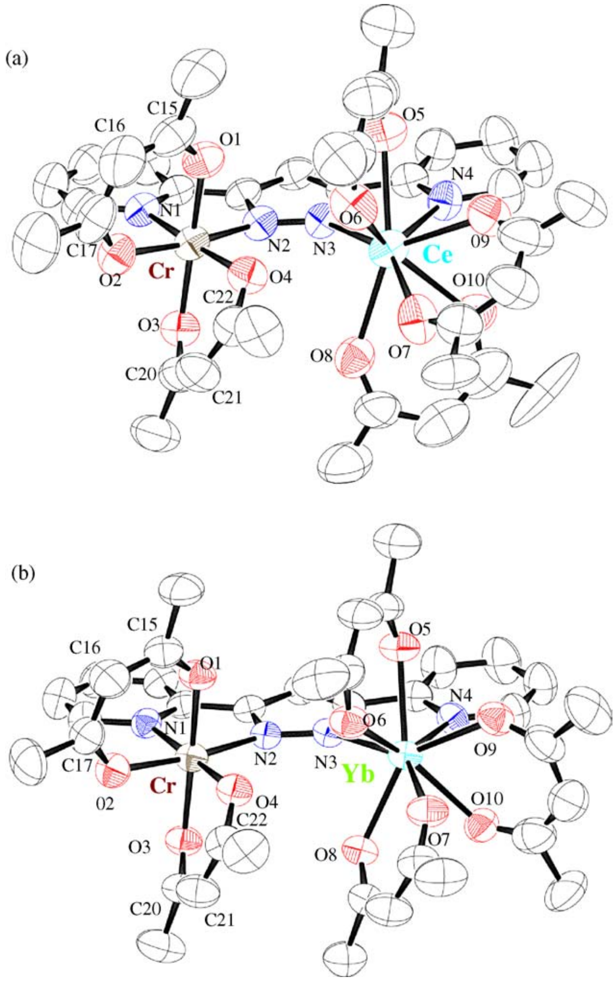

Fig. 1. ORTEP of **1** (a) and **7** (b).

2.2. *Crystal structure determination*

The measurements for the complexes **2**, **3**, **4**, **5** were made on a Rigaku AFC5R or 7R four-circle diffractometer with graphite monochromated Mo Kα radiation and a rotating anode generator. For the complexes **1**, **6**, **7**, a Rigaku Mercury CCD area detector was used with graphite monochromated Mo Kα radiation ($\lambda = 0.71070$) at 300 ± 1 K. Chemical formula, crystal systems, space group and no. of formula units in unit cell for the **1**–**7** complexes are summarized in Table 2.

3. Results and discussion

The complexes $[(hfac)_3Ln(\mu\text{-bpypz})Cr(acac)_2]$ crystallized to form violet (except brown for **1**(Ce)) cubic crystals

Table 2
Crystallographic data of the complexes **1**–**7**

Formula	Ce(**1**)	Nd(**2**)	Sm(**3**)	Gd(**4**)	Dy(**5**)	Er(**6**)	Yb(**7**)
M	1232.73	1236.85	1243.01	1249.86	1255.11	1259.87	1265.65
Crystal system	Monoclinic	Monoclinic	Monoclinic	Monoclinic	Monoclinic	Monoclinic	Monoclinic
Space group	$P2_1/c$	$P2_1/c$	$P2_1/c$	$P2_1/c$	$P2_1/c$	$P2_1/c$	$P2_1/c$
a (Å)	12.289(1)	12.354(7)	12.395(5)	12.441(4)	12.459(2)	12.4546(9)	12.4407(8)
b (Å)	17.472(2)	17.420(7)	17.36(1)	17.345(4)	17.330(2)	17.268(1)	17.230(1)
c (Å)	22.450(2)	22.385(7)	22.296(7)	22.274(2)	22.219(3)	22.126(2)	22.013(2)
β (deg)	95.020(4)	96.27(4)	97.11(3)	97.84(1)	97.97(1)	98.299(3)	98.322(3)
V (Å)	4801.9(7)	4788(3)	4761(3)	4761(2)	4751 (1)	4708.7(6)	4668.9(5)
Z	4	4	4	4	4	4	4
R_1 factor [$I > 3.0$ sigma (I)]	0.0669	0.0567	0.0545	0.0538	0463	0.0445	0393
R_w factor [$I > 3.0$ sigma (I)]	0.2140	0.2101	0.1971	0.1912	0.1680	0.1314	0.1056

Table 3
Selected bond lengths (Å), bonding angles (°) and torsion angles (°) of the complexes **1**–**7**

	Ce(**1**)	Nd(**2**)	Sm(**3**)	Gd(**4**)	Dy(**5**)	Er(**9**)	Yb (**7**)
Ln–O5	2.517(5)	2.471(5)	2.447(6)	2.430(6)	2.401(4)	2.378(4)	2.353(4)
Ln–O6	2.441(5)	2.399(5)	2.356(5)	2.339(5)	2.312(4)	2.288(3)	2.256(3)
Ln–O7	2.487(5)	2.438(5)	2.422(6)	2.391(6)	2.370(4)	2.356(3)	2.334(4)
Ln–O8	2.497(5)	2.459(4)	2.423(5)	2.394(5)	2.358(4)	2.329(3)	2.305(3)
Ln–O9	2.474(4)	2.424(5)	2.391(6)	2.364(5)	2.336(4)	2.312(3)	2.280(3)
Ln–O10	2.492(5)	2.473(4)	2.438(5)	2.405(5)	2.376(4)	2.360(3)	2.335(4)
Ln–N3	2.560(4)	2.526(4)	2.502(5)	2.493(5)	2.471(4)	2.455(3)	2.438(3)
Ln–N4	2.719(5)	2.667(5)	2.621(6)	2.597(6)	2.553(4)	2.513(4)	2.478(4)
Cr–O1	1.957(5)	1.940(4)	1.938(6)	1.952(5)	1.959(4)	1.961(3)	1.951(3)
Cr–O2	1.946(4)	1.948(4)	1.946(5)	1.944(5)	1.946(4)	1.942(3)	1.942(3)
Cr–O3	1.973(4)	1.968(4)	1.958(5)	1.967(5)	1.964(4)	1.962(3)	1.957(3)
Cr–O4	1.957(4)	1.952(4)	1.923(5)	1.933(5)	1.936(4)	1.930(3)	1.928(3)
Cr–N1	2.098(4)	2.098(4)	2.100(6)	2.091(5)	2.089(4)	2.091(4)	2.083(4)
Cr–N2	2.010(4)	2.010(4)	2.026(6)	2.046(5)	2.054(4)	2.063(3)	2.062(4)
Cr–N2–N3	133.2(3)	133.9(3)	134.7(4)	136.2(4)	137.1(3)	137.0(3)	137.7(3)
Ln–N3–N2	128.8(3)	131.1(3)	133.0(4)	134.2(4)	135.0(3)	136.1(2)	136.2(3)
O3–Cr–O4–C22	−41.5(4)	−39.5(4)	−36.0(6)	−34.6(5)	−32.3(4)	−31.8(3)	−31.1(4)
O4–Cr–O3–C20	34.8(5)	34.8(4)	32.4(6)	30.5(5)	29.1(4)	27.8(3)	28.0(4)

of the same space group $P2_1/C$. The molecular structures of complexes **1** and **7** with the atom numbering [14] are illustrated in Fig. 1. The small changes of the Cr–O4 bond lengths are found as shown in Table 3; being little shorter by ca. 1.5% from complex **1** to **7**, but the other Cr–O ones change to a much smaller extent. The Cr–N1 bond lengths are almost unchanged, but the Cr–N2 lengths become little longer by 2.5% from complex **1** to **7**. The bond lengths around Ln ions change according to the lanthanide contraction. The shortening of the Ln–O6 bond lengths from complex **1** to **7** is the largest by 7.6%. The Ce–N bond lengths change to a much larger extent than the other Ln–N ones as shown in Table 3; the Ln–N3 bond length by 4.5% and the Ln–N4 one by 9% from complex **1** to **7**. The X-ray structure of the complexes **1**–**7** demonstrated a discrete dinuclear Ln–Cr complex [13], two neighboring of which are π–π stacked with intermolecular distance (3.3–3.4 Å) between two bpypz planes. Each dinuclear complex has a distorted six coordinate octahedral OC–6 Cr^{III} and an eight coordinate bicapped trigonal prismatic TPRS–8 Ln^{III} configuration comprising two caps (O5 and O7) on the lateral faces (O9–O10–O8–O6 and O9–O6–N3–N4). One of three hfac chelates (O6–O5) and bpypz chelate (N3–N4) occupy the almost same positions in the TPRS for the complexes **1**–**7**, whereas the connections of the remaining two hfac chelates in **1** are different from those in **4**–**7**, demonstrating two kinds of the TPRS–8Ln^{III} configuration which are classified into the A and B forms (Scheme 1). Although the four oxygen ligators (O7, O8, O9, O10) of the two hfac chelates are located at the same vertices of the TPRS, the chelations between the O7 and O10 are interchanged: O8–O10 and O9–O7 for two hfac's in the complex **1** (A form). O7–O8 and O9–O10 for two hfac's in the complexes **4**–**7** (B form). For the Sm^{III}–Cr^{III} (**2**) and Nd^{III}–Cr^{III} (**3**) complexes, the X-ray analysis revealed a mixture of two disordered A

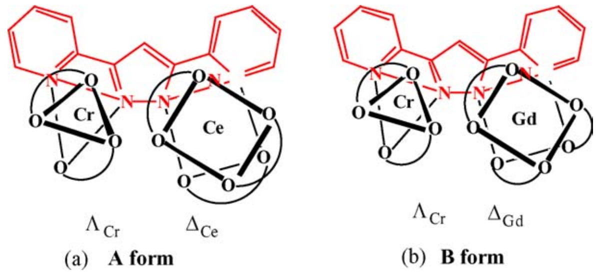

(a) **A form** (b) **B form**

Scheme 1. Schematic views of A form (a) and B form (b) with the configurational chirality definition.

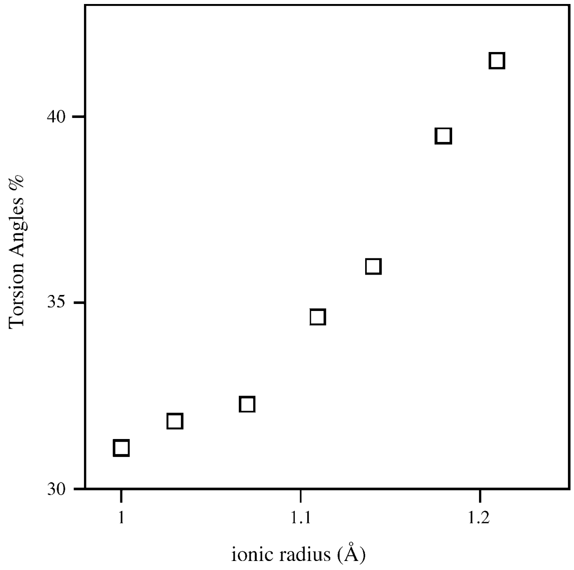

Fig. 2. A plot of torsion angles (O3–Cr–O4–C22) vs. ionic radius of Ln(III).

and B forms with about equal amounts. Thus, there occurs an unique ion size dependent structural transformation with configurational changes along the present series of Ln–Cr complexes. According to the definitions (Scheme 1) for the absolute configurations assuming the pseudo SAPR–8 Gd^{III} and OC–6 Cr^{III}, each two of four molecules in the unit cell have the Λ_{Cr}–Δ_{Ln} and Δ_{Cr}–Λ_{Ln} diastereomeric pairs, indicating diastereospecific assembly with configurational chilarity without asymmetric carbon as found for (Δ_{Cr}–Λ_{Ln})-[$(acac)_2Cr(\mu\text{-}ox)Ln(HBpz_3)_2$] [9,10]. Such a stereospecific configurational chiral assembling results from the difference in steric congestion of the acac and hfac chelates between the Δ_{Cr}–Λ_{Ln} (Δ_{Cr}–Λ_{Ln}) and Λ_{Cr}–Λ_{Ln} (Δ_{Cr}–Δ_{Ln}) complexes [15].

A series of the Cr–Ln dinuclear complexes **1**–**7** demonstrates another characteristic stereochemistry around the acetylacetonate chelate ring. One of the two acac chelates around Cr bends away from the proximate hfac chelate; the unusually larger torsion angles (O3–Cr–O4–C22) change gradually from the largest −41.5(4)° for the complex **1** to the smallest −31.1(4)° for the complex **7** (Fig. 2) as compared with that (8.8(5)° 9.3(4)°) for the other acac chelate (O2–Cr–O1–C15). As shown in Fig. 2, it is seen that the torsion angles become larger with increasing the Ln^{III} ion size, suggesting to synchronize the structural transformation from B to A form. Such a large bending in the acac chelate or structural transformation may result from steric requirement in the bridging moieties as inferred from shortening of nonbonding Ln···O4 distances from 3. 86 Å (**7**) to 3.16 Å (**1**) (Fig. 3) and/or triangular van der Waals contacts among O4, O6 and O8 or a π–π stacking between the hfac and acac in complexes **2** and **3** of the B form. Since there is no π–π stacking in the complex **1** of the A form even with the largest acac bending, this stacking does not necessarily bring about the bending. However, there is the intramolecular contact between CF_3 group of hfac in Ln^{III} and acac in Cr^{III} as in Fig. 4. Such a large bending in the acac chelate or structural transformation may result from steric requirement or congestion due to shortening of the interatomic distances or contacts in the bridging moieties as inferred from comparison of intramolecular structural parameters. That is, the decrease in nonbonding Ln···O4 distances (from 3.16 Å (**1**) to 3.86 Å (**7**)) and Ln···Cr distances (from 4.33 Å (**1**) to 4.65 Å (**7**) in Fig. 3) and/or counterbalance between the O4···O6 and O4···O8 distances with triangular van der Waals contacts among O4,

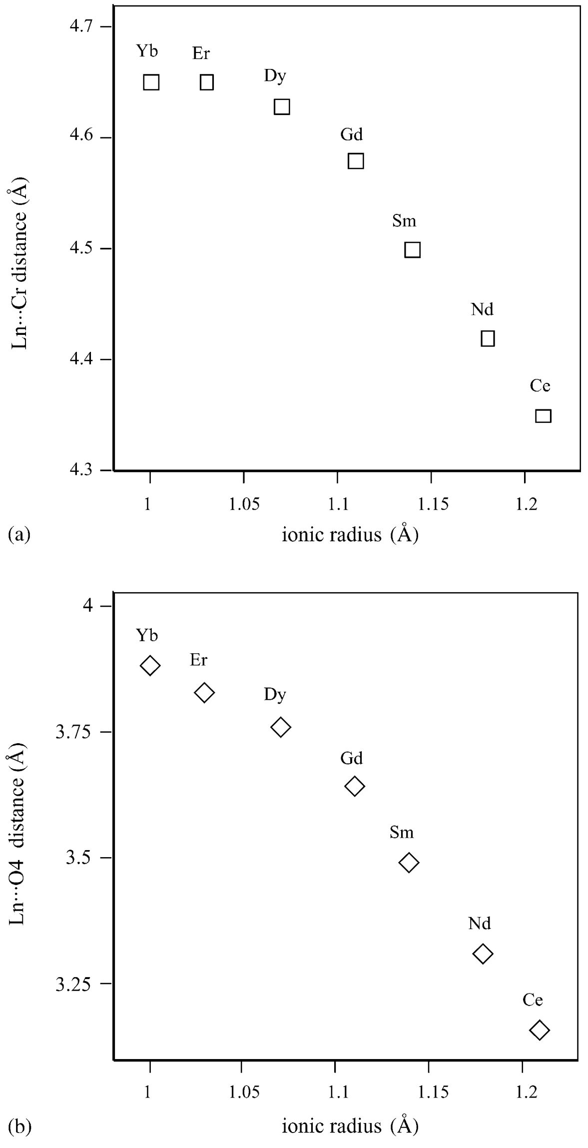

Fig. 3. Plots of ionic radius vs. Ln···Cr distance (a) and Ln···O4 distance (b).

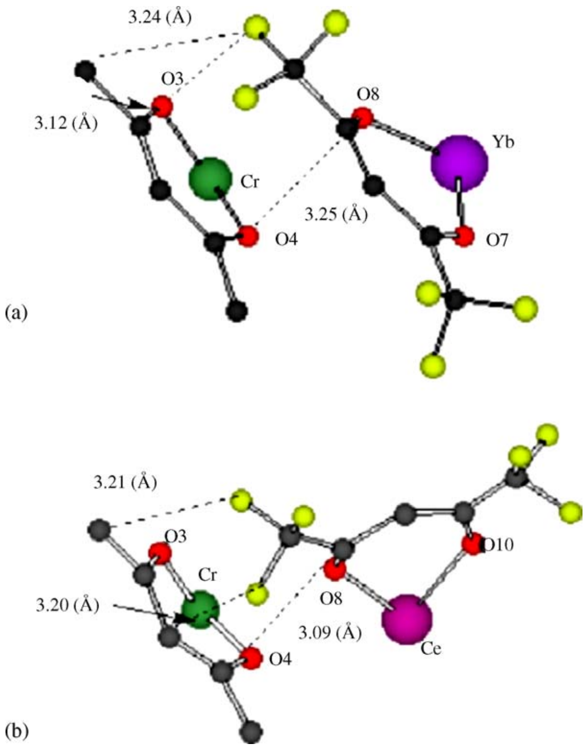

Fig. 4. Steric contact between the CF_3 group and acac in **1** (a) and **7** (b).

O6 and O8 are correlated with decreasing the ionic radius of Ln(III).

4. Conclusion

The geometrical environments or structural parameters of the bond lengths and angles around the bridging moiety for the complexes **2** and **3** are allowed to take both the A and B form where, in other words, the conformations for two forms would be almost equal in strain energy to each other. Otherwise, either the A or B form could be predominantly stabilized for the other complexes **1** or **4–7**. Such a drastic conformational transformation is tuned or controlled by the subtle difference in the Ln ion radius. It is noted that the Ln· · ·O4 distance also reflects the increasing tendency of the CN with increasing the $\mathrm{Ln^{III}}$ ion size as if there were an attractive force between Ln and O4. The analogous situation is encountered for $[(\mathrm{HBpz_3})\mathrm{Ln}(\mu\text{-}RS\text{-pba})_4\mathrm{Ln}(\mathrm{HBpz_3})]$ [5]. In this case, there is found the shortening of the Ln· · ·O nonbonding distance which is associated with increase of CN from **7** to **8** together with increasing ionic radius of Ln(III). For the present complexes, the shortening of the intramolecular nonbonding Ln· · ·O4 distance (Fig. 3) may be a driving force to transform the structure from A to B by inducing the shift of the van der Waals contact among O4, O6 and O8 with keeping steric contact between the CF_3 group of hfac and the acac chelate, associated with shortening the Ln· · ·Cr distance (Fig. 3) and decreasing the Ln–N3–N2 and N3–N2–Cr bond angles.

References

[1] D.R. van Staveren, G.A. van Albada, J.G. Haasnoot, H. Kooijman, A.M.M. Lanfredi, P.J. Nieuwenhuizen, A.L. Spek, F. Ugozzoli, T. Weyhermüller, J. Reedijk, Inorg. Chem. Acta 315 (2001) 163.

[2] S. Mizukami, H. Houjou, M. Kanesato, K. Hiratani, Chem. Eur. J. 9 (2003) 1521.

[3] F. Benetollo, G. Bombieri, L. Calabi, S. Aime, M. Botta, Inorg. Chem. 42 (2003) 148.

[4] T. Tsukuda, T. Suzuki, S. Kaizakai, J. Chem. Soc., Dalton Trans. (2002) 1721.

[5] M.A. Subhan, T. Suzuki, A. Fuyuhiro, S. Kaizaki, Dalton Trans. (2003) 3785.

[6] J.-C.G. Bünzli, C. Piguet, Chem. Rev. 102 (2002) 1897 (and the references therein).

[7] T. Sanada, T. Suzuki, S. Kaizaki, J. Chem. Soc., Dalton Trans. (1998) 959.

[8] T. Sanada, T. Suzuki, T. Yoshida, S. Kaizaki, Inorg. Chem. 37 (1998) 4712.

[9] M.A. Subhan, T. Suzuki, S. Kaizaki, J. Chem. Soc., Dalton Trans. (2001) 492.

[10] M.A. Subhan, T. Suzuki, S. Kaizaki, J. Chem. Soc., Dalton Trans. (2002) 1416.

[11] (a) M. Cantuel, G. Bernardinelli, D. Imbert, J.-C.G. Bünzli, G. Hofgartner, C. Piguet, J. Chem. Soc., Dalton Trans. (2002) 1929;
(b) M. Cantuel, G. Bernardinelli, J.P. Gilles Muller, Riehl, C. Piguet, Inorg. Chem. 43 (2004) 1840.

[12] C. Piguet, E. Rivara-Minten, G. Bernardinelli, J.-C.G. Bünzli, G. Hopfgartner, J. Chem. Soc., Dalton Trans. (1997) 421.

[13] R. Kawahata, T. Tsukuda, T. Yagi, Md. Abdus Subhan, H. Nakata, A. Fuyuhiro, S. Kaizaki, Chem. Lett. 32 (2003) 1084.

[14] Note that the atom numberings in the present paper are different from those in the previous one [13], but was right in the text.

[15] Note that the notations of the absolute configuration were wrong in Fig. 1 of the previous paper [13], but was right in the text.